Lossless Photonic Integrated Multicast Switch for Optical Wireless Data Center Network

Shaojuan Zhang, Netsanet Tessema, Xuwei Xue, Rafael Kraemer, Henrique Santana, Eduward Tangdiongga and Nicola Calabretta
Electro-optical Communications, Eindhoven University of Technology, 5600MB Eindhoven, The Netherlands
s.zhang4@tue.nl

Abstract: *We present an optical wireless data center network based on photonic integrated SOA based multicast switch (MCS) and arrayed waveguide grating router. Results show lossless and WDM MCS operation with <0.5dB power penalty at 10Gb/s.*
Keywords: *optical wireless technology, data center networks, fast optical switch*

I. Introduction

Boosted by the cloud computing paradigm, artificial intelligence, and the 5G applications, next-generation data center network (DCN) should be able to handle heterogeneous traffic volumes and satisfy the stringent requirements in terms of high bandwidth, low latency, high scalability, low cabling complexity, and high cost-power efficiency [1]. In traditional electrical switches based DCN with wired hierarchical tree-based architecture, the O/E/O conversions require costly and high power consumption dedicated interfaces [2]. Therefore, new technologies and architecture need to be investigated for the next-generation DCN. Optical switch DCN, featuring a high data rate and data format agnostic operation, has gained significant attentions [3]. However, the wired architecture still has low flexibility with cable complexity problems and cannot adapt to the bursty and changing requirements due to high latencies and slow reconfigurability. In this regard, introducing optical wireless technology into the next-generation DCN with optical switch technology is a promising solution.

The optical wireless DCN (OW-DCN) employing optical switch technology offers ultra-high data rates benefiting from the transparent switching capability of optical switch, as well as negligible waveguide dispersion and almost zero attenuation of free-space transmission. Moreover, it removes the cable complexity with plug-and-play wireless links, which provides a scalable and flexible architecture for fast reconfiguration and relocation. Several technologies have been employed for establishing an OW-DCN, such as MEMS [4], switchable mirrors [5], digital micro-mirror device [6], and Mechanically Steerable Links [7], or photonic integrated circuits with beam steering[8]. Those approaches suffer from high (milliseconds) switching time, resulting in low throughput and slow reconfigurability, leading to poor scalability and low efficiency. Besides, only numerical investigations or simple link experimental assessments have been reported in the aforementioned research.

In this paper, we propose and experimentally demonstrate a novel OW-DCN based on nanoseconds and lossless photonic integrated multicast switches (PIC-MCS) at the Top-of-the-Rack switches (ToRs) and arrayed waveguide grating routers (AWGRs). The data transmission between the ToRs is based on the wavelength mapping of the AWGR and realized by accordingly tuning on/off the corresponding transmission channels of the PIC-MCS. A 4×2 PIC-MCS has been designed, fabricated, and experimentally characterized. The system performance has been verified within a 4×4 racks DCN with 10G/s NRZ-OOK signals, which shows a lossless operation and successfully intra- and inter- cluster transmission with less than 0.5dB power penalty.

II. System operation of the OW-DCN

The architecture of the proposed OW-DCN with PIC-MCS and AWGR is depicted in Fig. 1(a). It has N clusters, and

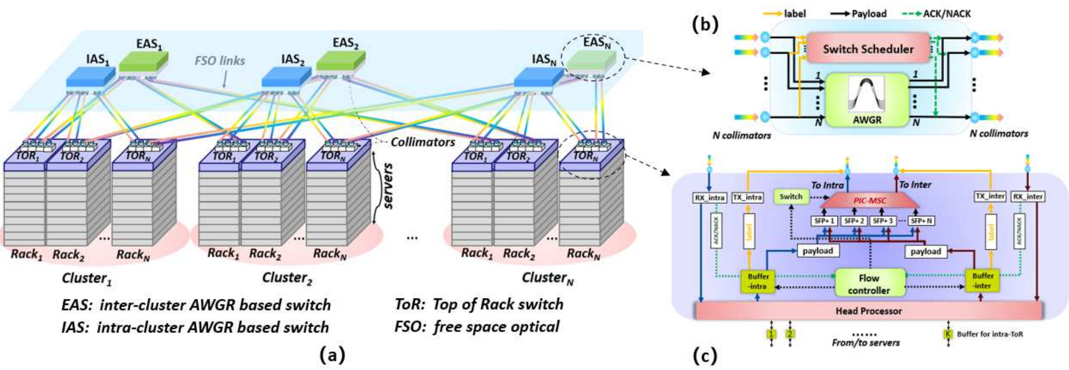

Fig. 1. (a) A schematic diagram of the OW-DCN architecture; (b) The functional blocks of the AWGR-based optical switch; (c) The functional blocks of PIC-MCS based ToR switch.

each cluster groups N racks. The N inter-cluster AWGR based switches (EAS) and N intra-cluster AWGR based switches (IAS) are dedicated for intra-cluster and inter-cluster communication between the racks, respectively. The functional block of this EAS or IAS is shown in Fig. 1(b). The fast switching of optical packets between ToRs is achieved by employing fast tunable transmitters and a passive AWGR. Table I shows the corresponding wavelength mapping of a $N\times N$ ports AWGR between each ToRs link. An FPGA-based switch scheduler is implemented to solve the potential contentions. For each transmission, an optical label signal is firstly generated by the FPGA-based ToRs and sent to the switch scheduler. An ACK or NACK control signal is then generated by the scheduler and sent back to the ToRs if the request is confirmed or rejected, respectively. On the ToRs side, the fast transmitters are implemented by FPGA-based ToRs and the PIC-MCS, as shown in Fig. 1(c). N SFP+ transceivers are directly plugged into the FPGA-based ToRs. The center wavelengths of these SFP+ are chosen accordingly as λ_1 to λ_N for matching the wavelength routing map of the AWGR. For each confirmed transmission, the FPGA-based ToRs firstly sends the electrical packet to the corresponding SFP+ according to the destination, and then switch the generated optical packet to the EAS or IAS by controlling the PIC-MCS. The AWGR-based EAS or IAS forwards the packet to the destination ToR via two free-space links constructed by two pairs of collimators. As for the rejected requests, retransmission is applied at the next time slot.

TABLE I. THE WAVELENGTH MAPPING OF A N×N PORTS AWGR.

AWGR	O1 (ToR1)	O2 (ToR2)	O3 (ToR3)	…	ON (ToRN)
I1 (ToR1)	λ0	λ1	λ2	…	λN
I2 (ToR2)	λ1	λ2	λ3	…	λ0
. . .	. . .	. . .	. . .	. . .	. . .
IN (ToRN)	λN	λ0	λ1	…	λ(N-1)

The schematic and the microscope image of the designed and fabricated 4×2 PIC-MCS is shown in Fig. 2(a) and (b). Signals that come from four input ports can be switched to any of the two output ports simultaneously via the eight transmission links established by 1x2 multimode interferometers (MMI) and quantum well active SOAs (employed as gates and amplifiers). To be specific, the optical signal coming from each input port is firstly spitted by one 1×2 MMI and fed into two SOA gates. The outputs of the SOA gates are then connected to two 4×1 combiners (based on cascaded 1×2 MMI). The outputs (O1 and O2) of the two 1×4 combiners direct the optical signals to the inter- and intra- cluster switch, respectively. Thus, turning on and off the SOA gates determines which signals are sent (multicasted) to the inter- and intra- cluster switch. A 1000-µm booster SOA is employed at each output port to compensate the on-chip splitting losses and fiber-to-chip coupling losses.

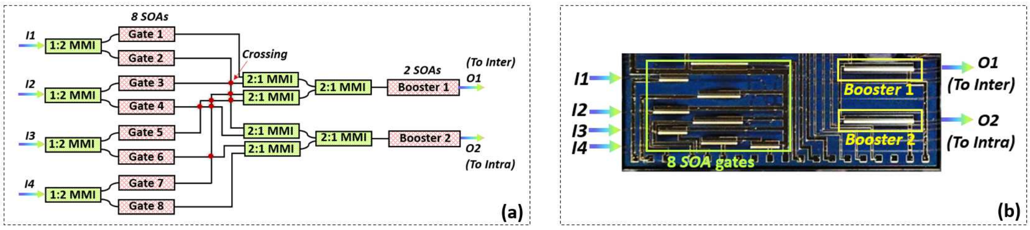

Fig. 2. (a) The schematic photonic integrated 4 × 2 MCS module; (b) The microscope image of the chip.

III. EXPERIMENTAL INVESTIGATIONS

The performance of the fabricated PIC-MCS is firstly characterized. The light-yellow electrodes of the on-chip SOAs are routed by on-chip metal tracks and then wire-bonded to the neighboring PCBs to enable the switch control or amplification. A water cooler is applied to maintain the chip at 20ºC. The fiber-to-fiber transmission gain is defined by comparing the received power at the fiber output port to the input power at the fiber input port. The 3 cascaded MMIs introduce around 10 dB losses, and the fiber-to-chip coupling loss is 6dB/facet. An input optical signal at 1551nm with power around 0 dBm is fed into input port 2 (I2) and switched out from output 2 (O2). The current of the booster SOA is set to 80 mA, while the gate (Gate 4) current varies between 0 mA (gate off) to 100 mA (gate on). Fig. 3(a) shows the fiber-to-fiber gain as a function of the current applied to Gate 5. The results indicate 2 dB net gain and higher than 37 dB on/off switching ratio from the chip for gate currents > 30mA. Besides, the performance under different input power is measured where the current of Gate 4 and the booster 2 are biased with 50 mA and 120 mA, respectively. The fiber-to-fiber gain, on/off switching ratio and output OSNR as a function of the input power have been measured in Fig. 3(b). It shows a fiber-to-fiber gain up to 7.9 dB, on/off switching ratio higher than 32 dB, and the output OSNR at least of 27 dB at low input powers. As it is observed, a lower gain is found for higher input power due to the SOA saturation. Moreover, the same performance assessments for the other optical paths have been measured for an input power of -2 dBm and show similar performance. The

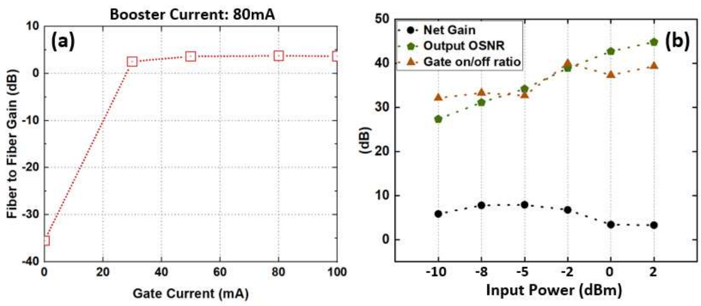

Fig. 3. (a) The fiber-to-fiber gain; (b) Performance of different input power.

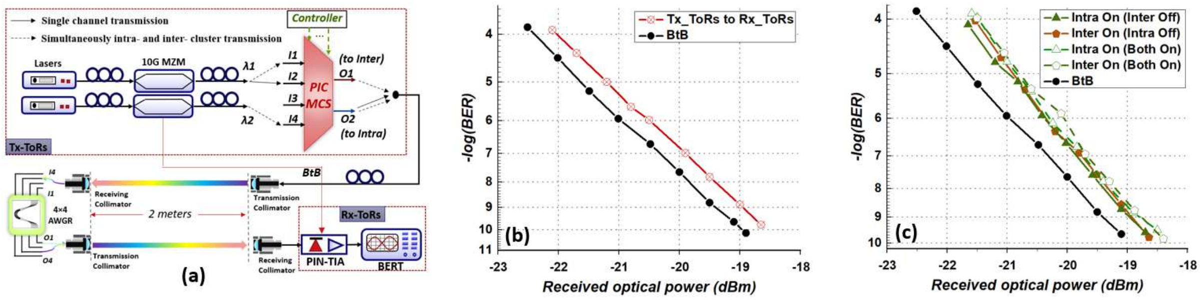

Fig. 4. (a) The experimental setup to assess the performance of the 2×4 PIC-MCS within a 4×4 racks DCN; (b) BER curves of the single-channel transmission; (c) BER curves of the intra- & inter- cluster transmission.

fiber-to-fiber gain ranged from 0.9 to 5 dB, switching on/off ratio is above 27 dB, and output OSNR is at least 33 dB.

The PIC-MCS and one 4×4 ports AWGR has been then employed in a proof-of-concept demonstration of one cluster with 4×4 racks OW-DCN as shown in Fig. 4(a). In order to assess the performance in different transmission scenarios, both single-channel transmission and simultaneously intra- and inter- cluster transmission have been assessed. According to Table I routing map, two lasers at 1547.75nm (λ_1) and 1549.34nm (λ_2) and two 10 Gb/s NRZ-OOK optical Mach-Zehnder modulators (MZM) are employed as optical transmitters for intra- and inter-cluster transmission, respectively. The PIC-MCS switches the optical data from the transmitters to the intra- or inter cluster free-space link to the AWGR. The AWGR works as the optical switch (EAS or IAS) to route the optical data to the destination ToRs. In order to evaluate the quality of the switched signals, bit error rate (BER) of the received data were measured. First, a single-channel transmission was evaluated by injecting the optical data signal at λ_1 to the input port 2 of the chip. The SOA Gate 4 and the SOA booster 2 operate with a current of 30 mA and 60 mA to switch the data signal to output port 2 with around -1 dBm output power. Meanwhile, more than 30 dB on/off switch ratio and over 44 dB OSNR were measured. Fig. 4(b) shows the BER curves after the free-space links and AWGR. A Back-to-Back (BtB) measurement is also included as reference. Results indicate error-free transmission operation with a power penalty of around 0.5 dB. Next, switching performance with both intra- and inter- channel transmission has been verified. In order to study the impact of the crosstalk, two data signals centered in λ_1 and λ_2 are injected to input port 1 and input port 4 to be switched to output 2 (intra-cluster transmission) and output 1 (inter-cluster transmission), respectively. These two paths have the highest number of waveguide crossings, as shown in Fig. 2(a). Therefore, two SOA gates (Gate 2 and Gate 7) and two SOA boosters (booster 1 and booster 2) are enabled simultaneously to switch the two signals in parallel. Fig. 4(c) shows the BER curves when both λ_1 and λ_2 optical data signals are switched as well as only one optical data is present and the other one is absent. Negligible crosstalk can be observed due to the simultaneous switching. Thus, a successful switching for both the intra- and inter- cluster transmission has been demonstrated, which validates the switching operation of the chip, and confirms the dynamic switch capability of the system.

IV. CONCLUSIONS

We have experimentally demonstrated an OW-DCN based on a novel photonic integrated MCS. The SOA based 4×2 PIC-MCS can provide fast switching as well as amplification for fiber-to-fiber gain. Switching performance with above 27 dB switching on/off ratio and at least 27 dB output OSNR were measured. Moreover, the PIC-MCS has been employed with a 4×4 port AWGR to validate the link performance of a 4×4 rack OW-DCN. Error-free operation at 10 Gb/s with <0.5 dB power penalty is achieved both for a single-channel and multi-channel transmission with negligible crosstalk interference.

REFERENCES

[1] W. Xia, P. Zhao, Y. Wen, and H. Xie, “A Survey on Data Center Networking (DCN): Infrastructure and Operations,” *IEEE Commun. Surv. Tutorials*, vol. 19, no. 1, pp. 640–656, 2017.

[2] X. Xue et al., “ROTOS: A Reconfigurable and Cost-Effective Architecture for High-Performance Optical Data Center Networks,” J. Light. Technol., vol. 38, no. 13, pp. 3485–3494, 2020.

[3] F. Yan, X. Xue, and N. Calabretta, “HiFOST: A scalable and low-latency hybrid data center network architecture based on flow-controlled fast optical switches,” J. Opt. Commun. Netw., vol. 10, no. 7, pp. B1–B14, 2018.

[4] P. Deng, M. Kavehrad, and Y. Lou, “MEMS-based beam-steerable free-space optical communication link for reconfigurable wireless data center,” Broadband Access Commun. Technol. XI, vol. 10128, no. January 2017, p. 1012805, 2017.

[5] N. Hamedazimi et al., “FireFly: A reconfigurable wireless data center fabric using free-space optics,” Comput. Commun. Rev., vol. 44, no. 4, pp. 319–330, 2015.

[6] M. Ghobadi et al., “ProjecToR: Agile reconfigurable data center interconnect,” SIGCOMM 2016 - Proc. 2016 ACM Conf. Spec. Interes. Gr. Data Commun., pp. 216–229, 2016.

[7] N. A. Riza, “The camceiver: Empowering robust agile indoor optical wireless for massive data centres,” 2019 42nd Int. Conf. Telecommun. Signal Process. TSP 2019, pp. 445–448, 2019.

[8] C. Chaintoutis et al., “Free space intra-datacenter interconnects based on 2D optical beam steering enabled by photonic integrated circuits,” Photonics, vol. 5, no. 3, 2018.